Available online at www.sciencedirect.com

ScienceDirect

Remote Sensing of Environment xx (2007) xxx–xxx

Remote Sensing of Environment

www.elsevier.com/locate/rse

Using MERIS full resolution data to monitor coastal waters — A case study from Himmerfjärden, a fjord-like bay in the northwestern Baltic Sea

Susanne Kratzer [a,*], Carsten Brockmann [b], Gerald Moore [c]

[a] *Department of Systems Ecology & Department of Physical Geography and Quaternary Geology, Stockholm University, SE-106 91 Stockholm, Sweden*

[b] *Brockmann Consult, Max-Planck-Str. 2, D-21502 Geesthacht, Germany*

[c] *Plymouth Marine Laboratory (PML), Prospect Place, Plymouth PL1 3DH, UK*

Received 30 October 2006; received in revised form 19 October 2007; accepted 19 October 2007

Abstract

In this paper we investigate if MERIS full resolution (FR) data (300 m) is sufficient to monitor changes in optical constituents in Himmerfjärden, a fjord-like, north–south facing bay of about 30 km length and 4 km width. The MERIS FR products were derived using a coastal processor (FUB Case-2 Plug-In). We also compared the performance between FUB and standard processor (MEGS 7.4), using reduced resolution (RR) data (1 km resolution) from the open Baltic Sea, and compared the products to sea-truthing data. The optical variables measured for sea-truthing were chlorophyll, suspended particulate matter (SPM), as well as coloured dissolved organic matter (CDOM, also termed yellow substances), and the spectral diffuse attenuation coefficient, $K_d(490)$. The comparison of the RR data to the sea-truthing data showed that, in the open Baltic Sea, the MERIS standard processor overestimated chlorophyll by about 59%, and SPM by about 28%, and underestimated yellow substance by about 81%, whereas the FUB processor underestimated SPM by about 60%, CDOM by about 78%, and chlorophyll *a* by about 56%. The FUB processor showed a relatively high precision for all optical components (standard deviation: 6–18%), whereas the precision for the MEGS 7.4 was rather low (standard deviation: 43–73%), except for CDOM (standard deviation: 13%). The analysis of the FR data showed that all FR level 2 water products derived from MERIS followed a polynomial decline in concentration when moving off-shore. The distribution of chlorophyll and SPM was best described by a 2nd order polynomial, and the distribution of CDOM by a 3rd order polynomial, verifying the diffusional model described in Kratzer and Tett [Kratzer, S. and Tett, P. (in press). Using bio-optics to investigate the extent of coastal waters — a Swedish case study. Hydrobiologia.]. A new $K_d(490)$ and Secchi depth algorithm based on MERIS channel 3 (490 nm) and channel 6 (620 nm) each was derived from radiometric sea-truthing data (TACCS, Satlantic). Applying the $K_d(490)$ algorithm to the MERIS FR data over Himmerfjärden, and comparing to sea-truthing data the results showed a strong correlation ($r=0.94$). When comparing the FR data to the sea-truthing data CDOM and $K_d(490)$ showed a low accuracy, but a high precision with a rather constant off-set. In summary, one may state that the precision of MERIS data improves by applying the FUB Case-2 processor and the accuracy improves with improved spatial resolution for chlorophyll and SPM. Furthermore, the FUB processor can be used off-the-shelf for open Baltic Sea monitoring, provided one corrects for the respective off-set from sea-truthing data which is most likely caused by an inaccuracy in the atmospheric correction. Additionally, the FR data can be used to derive CDOM, $K_d(490)$ and Secchi depth in Himmmerfjärden if one corrects for the respective off-set. We will need to perform more comparisons between sea-truthing and MERIS FR data before the new $K_d(490)$ algorithm can be made operational, including also scenes from other times of year. In order to provide a level 2 product that can be used reliably by the Baltic Sea user community, our recommendation to ESA is to include the spectral attenuation coefficient as a MERIS standard product.

Keywords: MERIS FR data; Baltic Sea; Coastal zone; Spectral diffuse attenuation coefficient, $K_d(490)$; Secchi depth; Algorithm development

1. Introduction

Before the advance of satellite remote sensing, physical oceanographers had studied the optical properties of the oceans for several decades. The pioneer work was done by Jerlov

* Corresponding author.
E-mail address: susanne.kratzer@ecology.su.se (S. Kratzer).

0034-4257/$ - see front matter © 2007 Elsevier Inc. All rights reserved.
doi:10.1016/j.rse.2007.10.006

during the Swedish deep-sea expedition in 1947–1948. Jerlov measured spectral diffuse attenuation coefficients across the world's oceans (Jerlov, 1951). This resulted in Jerlov's optical classification into the oceanic water types I (the clearest natural waters), II, III and the coastal water types 1–9 (Jerlov, 1976). In the late 1970 ties Morel and Prieur (1977) developed a new optical classification of natural water bodies, dependent on the concentrations of optical in-water constituents. Waters in which the optical properties are dominated by factors other than phytoplankton, and their products are defined as optical Case-2 waters. In these waters, which are generally coastal waters, coloured dissolved organic matter (CDOM, also termed yellow substance) or suspended particulate matter (SPM) may play an important part in light attenuation, in addition to the part played by water itself and phytoplankton pigments.

There have been many studies to develop remote sensing algorithms to estimate the chlorophyll concentrations (used as a proxy for phytoplankton biomass) in clear waters. Most of these algorithms are based on colour ratios, such as the blue-green ratio (Gordon & Morel, 1983), which are empirically related to the chlorophyll *a* concentration. Using ratios it is possible to eliminate unwanted effects such as absolute calibration errors, and therefore they are a suitable tool for remote sensing. However, in optical Case-2 waters, this empirical approach does not work, and the same algorithms can not be applied as there are two or more substances present, which have different spectral properties and do not necessarily co-vary with chlorophyll *a* concentration (Mueller & Austin, 1995). The presence of high concentrations of CDOM and/or SPM leads to significant problems when applying simple algorithms for the retrieval of chlorophyll in Case-2 waters. Generally, waters with a CDOM absorption above 0.1 m^{-1} at 380 nm (corresponding to a CDOM absorption of about 0.03 m^{-1} at 440 nm) and/or SPM concentrations above 0.5 gm^{-3} may be classified as Case-2 waters, and in practice, only those water types for which the blue-green ratio algorithms for chlorophyll concentration can be applied have been treated as Case-1.

In the early 60 ties, Preisendorfer introduced a system which separated optical properties into two categories — inherent and apparent (Preisendorfer, 1961). Apparent optical properties (AOPs), e.g. radiance and irradiance, are those affected by a change in the radiance distribution, while inherent optical properties (IOPs) are independent of changes in the radiance distribution and depend only on the substances within the aquatic medium. The IOPs are the absorption and the scattering coefficients, and the volume scattering function, $\beta(\theta)$, which is the angular variation of scattering. The reflectance of sea water is proportional to the ratio of backscattering to absorption at a given wavelength (Kirk, 1994; Morel & Gentili, 1991, 1993, 1996):

$$R \approx f\ b_b\ (a + b_b)^{-1}$$

(Gordon, 1973; Morel & Gentili, 1991, 1993, 1996; Sathyendranath & Platt, 1997).

The new generation of ocean colour satellites (e.g. SeaWiFS, MODIS, MERIS) have a high radiometric resolution, which means they are especially adapted to the low radiances of aquatic ecosystems. The spatial resolution of ocean colour satellites is, however, usually only about 1 km, which means that the satellite does not show variability at a small, local scale, and therefore is not adequate for monitoring coastal areas. With its improved spatial resolution of 300 m the European Space Agency's sensor MERIS on the ENVISAT-1 satellite is the first ocean colour sensor that is adequate for coastal remote sensing (Doerffer et al., 1999). It also has an improved spectral resolution, with 15 programmable spectral bands. The MERIS Case-2 water algorithm is a neural network (NN), which uses the logarithm of the remote sensing reflectance above the surface of eight of the fifteen MERIS bands after atmospheric correction (Doerffer & Schiller, 2006). The eight bands used for deriving the level 2 products are centered at 412, 442, 490, 510, 560, 620, 665 and 708 nm. Furthermore, solar and viewing zenith, as well as azimuth difference are required as input to the NN. The output of the NN is the logarithm of the following three IOPs: pigment absorption at 442 nm (a_{ph}442), the summed-up absorption of yellow substance and bleached suspended matter, $a_{dg}(442)$ and the scattering coefficient of all suspended particulate matter at 442 nm, $b_p(442)$. The IOPs are then used to derive the concentration of chlorophyll *a* and total suspended matter (dry weight), which together with the yellow substance absorption, form the three Case-2 water products of MERIS. Note that the actual MERIS product for yellow substance is YSBPA (the summed-up absorption of yellow substance and the bleached particle absorption, BPA, measured with the filter pad method at 440 nm, MERIS protocols: Doerffer, 2002). However, in the Baltic Sea, the yellow substance absorption is much greater than the bleached particle absorption ($a_{CDOM}442 \gg a_{BPA}442$), and therefore we treat the YSBPA product as a YS product (which would be equivalent to the SeaWiFS CDOM product).

By using the inverse of the respective conversion factors, it is possible to go back one step, and compute the three IOPs (a_{ph}442, $a_{dg}(442)$ and $b_p(442)$) from the derived products again, which may be useful if one wants to apply a local conversion factor for a specific coastal area. The NN is trained with about 30 000 simulated R_{rs} spectra, covering a large range from optical Case-1 to Case-2 waters. The simulation of the R_{rs} spectra is performed using the *Hydrolight* radiative transfer model. MERIS is currently in its calibration and validation phase, and the work presented here is aimed at validating MERIS in northwestern Baltic waters.

One of the greatest challenges for reliable retrieval of optical parameters over Case-2 waters is the reliable atmospheric correction. Automated procedures to derive aerosol concentration from ocean colour sensors over optical Case-1 waters using the dark pixel correction (Antoine & Morel, 2000; Gordon & Wang, 1994), which assume zero water-leaving radiance in the near-infrared, are not suitable for optical Case-2 waters, and tend to lead to negative water-leaving radiance in the blue. The remote sensing of optical Case-2 waters, however, requires new approaches for the atmospheric correction of the data as there are no wavelengths in the reflectance spectra where the water-leaving radiance is zero. The atmospheric correction of MERIS data over Case-2 waters is therefore based on the bright pixel approach which is described in the Algorithm Theoretical Basis Document, ATBD 2.6 (Moore & Aiken, 2000), and uses the reflectances at MERIS channel 12 (778 nm) and channel 14 (885 nm). Another attempt to solve the atmospheric correction is the neural network approach described by Schroeder et al. (2002). There are also several coupled ocean-atmosphere models in development that include both an atmospheric correction model, as well as a bio-optical in-water model that can be tuned to local conditions (Moore et al., 1999; Stamnes et al., 2003; Lavender et al., 2005).

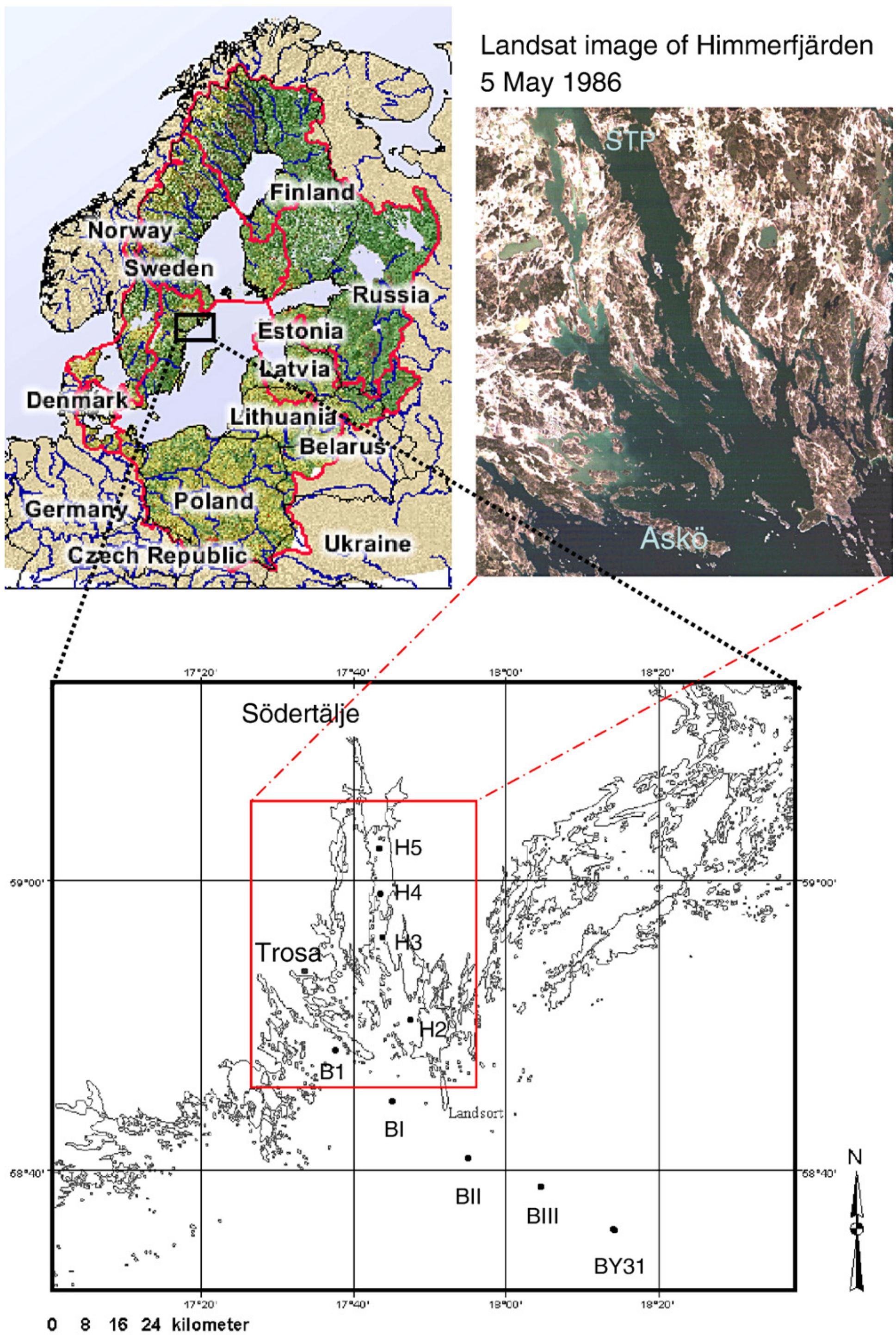

Fig. 1. Upper left: map of the Baltic Sea (from: http://maps.grida.no/baltic/) with the area of investigation indicated as a black box. Note the slight fluvial input on the northwestern compared to the southern Baltic Sea coast. Upper right: Landsat image of Himmerfjärden from 5 May 1986, the sewage treatment (STP) is situated at the head of Himmerfjärden, and Askö Laboratory on Askö, the Island at the mouth of Himmerfjärden. The transect locations are marked on the lower map. The outlet of the Himmerfjärden STP is situated close to location H5, at the head of Himmerfjärden. BY31 is at Landsort Deep, the deepest part of the Baltic Sea (459 m).

Please cite this article as: Kratzer, S., et al., Using MERIS full resolution data to monitor coastal waters — A case study from Himmerfjärden, a fjord-like bay in the northwestern Baltic Sea, *Remote Sensing of Environment* (2007), doi:10.1016/j.rse.2007.10.006

1.1. Area description

The Baltic Sea may be regarded as an inland sea or as a large fjord of the Atlantic Ocean with weak tides (<20 cm) and in most places broad shallow margins. It is characterised by a permanent salinity stratification with a brackish surface layer caused by the high freshwater input from rivers and more saline deep and bottom waters coming in from the North Sea. In the Baltic Proper the halocline ranges between 40 and 70 m depth. During spring and summer, a thermocline develops at depths between 15 and 20 m in most parts of the Baltic Sea, providing another density barrier for vertical exchange (Voipio, 1981). Apart from vertical density stratification, the high fluvial input from the north and the saline input of water from the North Sea also produce a strong horizontal salinity gradient across the whole Baltic Sea. The surface salinity decreases progressively from 6–8 in the Baltic Sea proper, to 5–6 in the Bothnian Sea, down to 2–3 in the Bothnian Bay. The salinity is therefore low compared to other seas, and the large freshwater content is associated with a high content of coloured dissolved organic matter. Because of the low tidal range, and the strong salinity stratification, there is relatively little resuspension of sediments. From the point of view of remote sensing, the Baltic Sea comprises optical Case-2 waters. Because of the high freshwater input and the little exchange with the North Sea, the open Baltic Sea is optically dominated by coloured dissolved organic matter (Darecki & Stramski, 2004; Kratzer, 2000; Kratzer et al., 2003), which has been shown to be inversely related to salinity (Bowers et al., 2000; Højerslev et al., 1996; Kratzer et al., 2003; Siddorn et al., 2001). In the southern Baltic Sea, the high fluvial input leads to sediment plumes with high sediment loads. However, compared to this, the northwestern Baltic Sea has relatively low sediment run-off (Kratzer & Tett, in press).

1.2. Site description

Himmerfjärden is a fjord-like bay situated in the Southern Stockholm Archipelago, just south of 60° N, opening into the Baltic Sea (Fig. 1). There is little fluvial input in this northwestern part of the Baltic Sea. With a mean depth of about 17 m Himmerfjärden is rather shallow and consists of a sequence of basins divided by several sills. Due to the low freshwater input (flushing rate 0.025 d^{-1}) and the presence of several sills Himmerfjärden has a weak circulation, and water residence times have been estimated to be upwards of 20 days (Engqvist, 1996), increasing with water depth and distance to the mouth of Himmerfjärden. Kratzer and Tett (in press) have shown that, theoretically, the distribution of particles or dissolved matter along a gradient perpendicular to the coast can be described as a low order polynomial if one uses diffusion theory as the driving force for the distribution of particles. Analysing transects of all three main optical constituents from Himmerfjärden it was shown that all optical constituents indeed could be best described by a polynomial. The distribution of chlorophyll and SPM was best described by a 2nd order polynomial (for chlorophyll there was no significant difference in applying a 1st or second order polynomial), and the distribution of CDOM by a 3rd order polynomial, with high concentrations in the coastal areas and low variability in the open sea.

1.3. Aim of this study

Earlier remote sensing work with SeaWiFS (Kratzer et al., 2003) had shown that the spatial resolution of SeaWiFS (1.1 km) was not sufficient to monitor water quality inside Himmerfjärden. The aim of this study is to investigate:

I. If MERIS FR data has a good enough spatial resolution to monitor changes in optical variables in Himmerfjärden; and
II. If the level 2 data (geophysical parameters such as chlorophyll, CDOM and SPM) derived from MERIS full resolution data (300 m spatial resolution) also show a polynomial decline when moving from a terrestrial source to an open sea sink as shown by the coastal diffusion model described in Kratzer and Tett (in press);
III. Furthermore, we will use sea-truthing data to develop new $K_d(490)$ and Secchi depth algorithms for MERIS. We will also apply the new $K_d(490)$ algorithm to MERIS FR data over Himmerfjärden, and test how well the satellite-derived data compares to measured data (using a different MERIS scene).
IV. We will also compare the performance of the MERIS standard processor to the *MERIS Case-2 Water Properties Processor* developed at the Freie Univesität Berlin (FUB) and described by Schroeder and Schaale (2005), using RR data.

2. Methods

2.1. Sea-truthing

In order to verify and test MERIS FR data over coastal waters we investigated an optical transect (about 58 km in length) from the head of Himmerfjärden to a station in the Landsort Deep in the deepest part of the Baltic Sea (Fig. 1) with a seabed depth of 459 m. Hence, the transect data covered an inshore to off-shore gradient to aim at a wide range of values for physical, biological and optical variables. Table 1 shows the dates, locations and station numbers for the sampled transects. Besides being aimed at sea-truthing, the optical data measured

Table 1
Dates and location for all optical transect stations in 2002, see also Fig. 1

Date	Transect	Location	Station I.D.
09-08-2002	Open Baltic	BY31′ – BIII’ – BII’ – BI’	2a – 2b – 2c – 2d
12-08-2002	Himmer-fjärden	H5 – H4 – H3 – H2	3a – 3b – 3c – 3d
15-08-2002	Open Baltic	BY31 – BIII – BII – BI – Persö	4a – 4b – 4c – 4d – 4e
22-08-2002	Himmer-fjärden	H5 – H4 – H3 – H2	7a – 7b – 7c – 7d

was also used to test a diffusional model of the coastal zone (Kratzer & Tett, in press, Fig. 2).

The information for the MERIS overpasses was requested from ESA during the planning phase of the field campaign. A sea-truthing transect consisted usually of 4–5 stations (Table 1), with 20 min sailing between stations and 40 min sampling and measuring at each station. The measurements of optical properties of the water were timed with MERIS overpasses +/−2 h. Furthermore, near real-time quick-looks were provided from the SeaWiFS project by the automated SeaWiFS Data Processing System (SDPS, NASA). The level 1 quick-looks were jpeg files of “true colour” images (bands 6,5,1, Fig. 3a) and level 2 quick-looks were gif files (chlorophyll concentration, Fig. 3b), which were sent by e-mail on a daily basis. This information helped to decide on sampling strategies during field campaigns, as the MERIS protocols (Doerffer, 2002) require a homogeneously mixed water body for calibration and validation of imagery, which meant that surface accumulations of filamentous cyanobacteria had to be avoided.

Geophysical and optical variables were measured at these stations during field campaigns in August 2002. GPS positions (GARMIN, GPSMAP, datum: WGS-84) were recorded for each station, and used to calculate distances from the waste water discharge of Himmerfjärden sewage treatment plant.

The spectral attenuation coefficient, $K_d(490)$ was estimated using a radiometric system (TACCS, Satlantic Inc., http://www.satlantic.com/) that included a chain of four sensors for downwelling irradiance at 490 nm, $E_d(490)$, with 10 nm bandwidth. The $E_d(490)$ sensors were fixed on a cable at 2, 4, 6 and 8 m depth ($K_d(490)$ chain).

The instrument was set to record for 2 min at a rate of 1 sample per second, having first been allowed to float 10–20 m away from the boat in order to avoid shading. The data was converted from binary to calibrated engineering units using the Satlantic SatCon software. The natural logarithm of the measured downwelling irradiance was plotted against depth and the slope of the line taken as $K_d(490)$.

The multi-channel radiometer also included 7 channels for upwelling radiance, L_u (unit: μW cm^{-2} nm^{-1}sr^{-1}), consisting of the 6 visible SeaWiFS channels plus an additional channel at 620 nm, and 3 channels for downwelling irradiance, E_d (unit: μW cm^{-2} nm^{-1}, above the surface) at about 443, 491 and 670 nm. In order to derive reflectance from the TACCS data, we first derived the spectral shape of the diffuse attenuation-given that we only had a measure of $K_d(490)$ derived from the K_d chain. This was done by using AC9 data measured during 2001–2002 (Kratzer et al., in preparation). The AC9 data was corrected for salinity and temperature, and processed according to WetLabs method 2, which assumes that the scattering correction is a fixed proportion of the scattering coefficient (WetLabs, 2007). Spectral scattering was derived as difference between spectral beam attenuation, c and spectral absorption, a for all AC9 channels, i.e. 412 nm, 440 nm, 488 nm, 510 nm, 532 nm, 555 nm, 630 nm, 676 nm, and 715 nm.

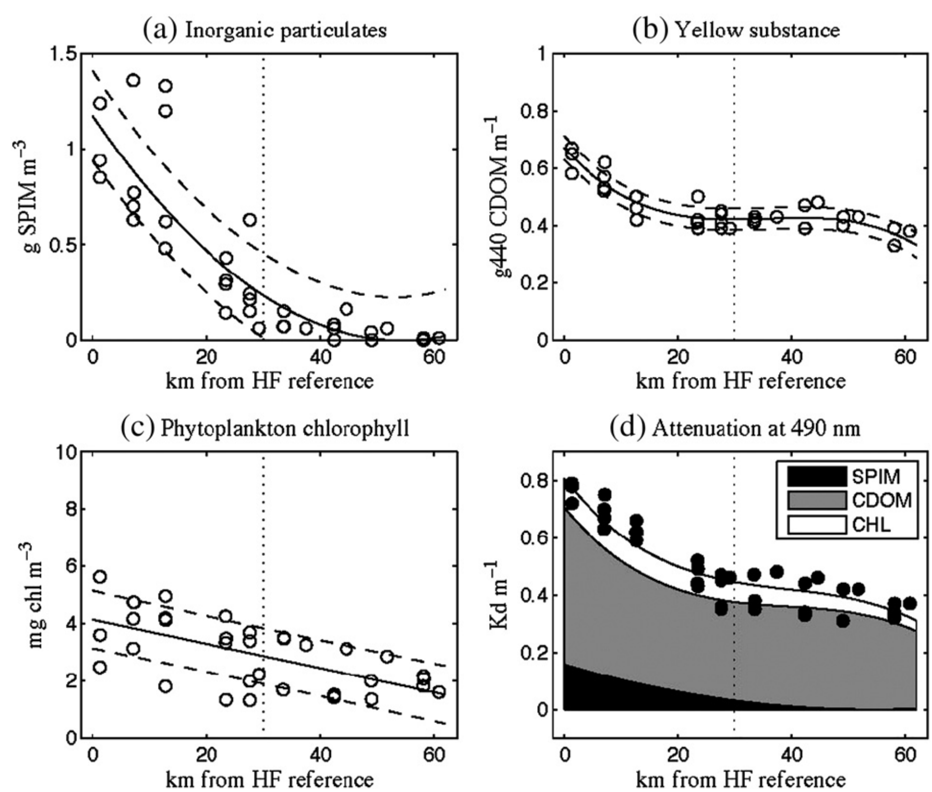

Fig. 2. Coastal model as developed in Kratzer and Tett (in press). The model illustrates the stacked contributions of each optically active component to $K_d(490)$ assuming a polynomial decline of optically active constituents in relation to the source (land), in this case we used the outlet of the Himmerfjärden (HF) sewage treatment plant as a nominal starting point of the transect.

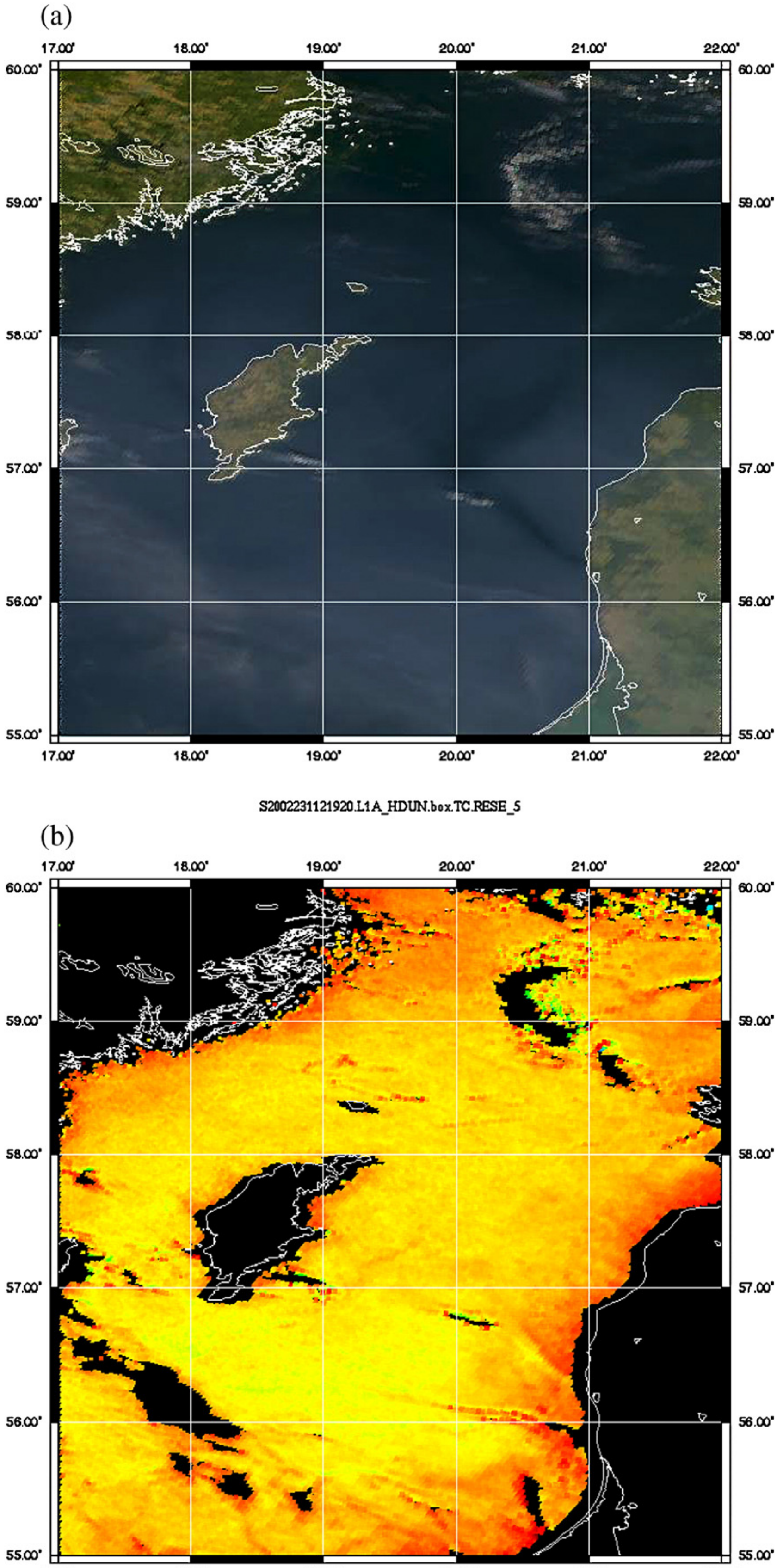

Fig. 3. Near real-time quick-looks as provided by the SeaWiFS project by the automated SeaWiFS Data Processing System (SDPS, NASA). The quick-looks were (a) jpeg files for "true colour" images (from level 1 data, bands 6,5,1), and (b) gif files for level 2 data (chlorophyll concentration), which were sent by e-mail on a daily basis. Note that the quick-looks only gave relative changes in chlorophyll concentrations, but they proved to be useful in deciding over the sampling strategies.

Please cite this article as: Kratzer, S., et al., Using MERIS full resolution data to monitor coastal waters — A case study from Himmerfjärden, a fjord-like bay in the northwestern Baltic Sea, *Remote Sensing of Environment* (2007), doi:10.1016/j.rse.2007.10.006

For deriving spectral K_d we first derived a and b at TACCS channels by linear interpolation between the AC9 channels (TACCS channel at 443 nm, 488 nm, 630 nm, and 676 nm). Then we used the following algorithm from Kirk (1994), that allows us to estimate spectral K_d from spectral a (absorption) and b (scattering):

$$K_d = \mu_0^{-1}\left[a^2 + (g_1 * \mu_0 - g_2)a * b\right]^{0.5} \qquad \text{(Kirk, 1994)}$$

Assuming a cosine of the refracted solar beam just below the surface $\mu_0=0.86$; and the constants $g_1=0.425$ and $g_2=0.19$. Table 2 shows the spectral K_d slopes derived from the AC9 data (Kratzer et al., in preparation). The data set was divided up into I) outer fjord & open sea stations (B1–BY31 & H2), and II) inner fjord stations (H3–H4). The reflectance, ρ (rho), was then estimated from the TACCS radiometer in the following way. The upwelling radiance just below the surfaces was estimated from the upwelling radiance at 50 cm depth by propagating each reading to the surface using the estimated K_d values for each radiance channel. The radiance above the surface was then derived from the upwelling radiance below the surface by multiplying the radiance values with a factor of 0.547 (Mueller & Austin, 1995). Then, the reflectance, ρ (rho), was estimated from the ratio of upwelling radiance and downwelling irradiance, multiplied by the factor ϕ (PI=3.14159).

2.2. Algorithm development

In SeaDAS (SeaWiFS data analysis system), $K_d(490)$ is derived from normalized water-leaving reflectance (L_{wN}) or reflectance (ρ_w) (Mueller, 2000), using band ratio algorithms of the following form: $K_d\ (490)=K_w\ (490)+A\ [L_{wN}\ (\lambda_1)/L_{wN}\ (\lambda_2)]^B$, where: K_w (490) is the diffuse attenuation coefficient for pure water, and λ_1, λ_2 are two wavebands, in the case of CZCS $\lambda_1=443$ nm and $\lambda_2=550$ nm, and in the case of SeaWiFS $\lambda_1=443$ nm and $\lambda_2=555$ nm. The 550 or 555 nm band is the low absorption, reference band. The A and B coefficients are determined from empirical fits to sea-truthing data, predominately clear ocean waters in the case of Mueller (2000).

Because $K_d(490)$ is not a standard level 2 product of MERIS data we derived our own $K_d(490)$ algorithm from our TACCS radiometer. For this, we used additional data that was sampled in between the transect dates (Table 1), so we had a total number of 23 $K_d(490)$ and reflectance measurements from 2002. The measured diffuse attenuation coefficients were first corrected by subtracting 0.022 m^{-1}, the diffuse attenuation of pure seawater at 490 nm, K_w (Smith & Baker, 1981). Then the natural logarithm of all combinations of reflectance ratios were regressed against ln $[K_d(490)-K_d w]$. The combination of reflectance ratios that scored the highest coefficient of determination, i.e. 490:620, was chosen for the final algorithm. In order to derive a Secchi depth algorithm the natural logarithm of the Secchi depth was related to various combinations of ln-transformed colour ratios, and the best Secchi algorithm was chosen in the same way. In order to test the robustness of the derived algorithms we also included data from cruises in 2000 and 2001 that was measured with the same protocol.

2.3. Water samples

The concentration of organic and inorganic SPM was measured in triplicates by gravimetric analysis using the method of Strickland and Parsons (1972). For the determination of CDOM the water was filtered through 0.22 µm membrane filters and measured spectrophotometrically (300–800 nm) in a 10 cm optical cuvette using a Shimadzu UVPC 2401 spectrophotometer. The optical density (OD), i.e. absorbance, at 440 nm was corrected for the OD at 750 nm, and G_{440}, the absorption coefficient for CDOM at 440 nm, was derived as follows:

$$G_{440} = \ln(10) \times (\mathrm{OD}_{440} - \mathrm{OD}_{750})/L\ \left(m^{-1}\right), \qquad \text{Kirk (1994)},$$

where L is the path length of the cuvette in meters (in this case 0.1 m).

For the estimation of photosynthetic pigments the spectrophotometric method was used (Jeffrey & Humphrey, 1975; Jeffrey et al., 1997; Parsons et al., 1984), using GF/F filters and extraction into 90% acetone. Chlorophyll *a* was calculated according to the trichromatic method (Parsons et al., 1984). All laboratory methods followed a standard protocol (Kratzer, 2000; Kratzer & Tett, in press; Kratzer et al., 2000).

2.4. Processing of satellite data

Two MERIS full resolution (FR) images (300 m resolution) from 19 and 22 August 2002 respectively were analysed. For the 22 August 2002, we had a matching sea-truthing transect through Himmerfjärden (station 7a, 7b, 7c, 7d, see Table 1).

The level 1b processor for the MERIS FR data was the operational ESA processor (IPF 4.10), and for level 2 processing the 'MERIS Case-2 Water Properties Processor' developed at the Freie Univesität Berlin (Schroeder & Schaale, 2005), herein referred to as 'FUB Case-2 Plug-In', was used to derive the concentration of chlorophyll *a*, SPM (total suspended

Table 2
Mean slope factors to derive spectral K_d for all TACCS channels from K_d490 in the northwestern Baltic Sea during summer (Kratzer et al., in preparation)

TACCS Band	Slope factors, outer stations, B1–BY31 & H2		Slope factors, inner fjord, H3–H4	
Wavelength, nm	Mean	SD	Mean	SD
412	2.424	0.17	2.043	0.10
443	1.673	0.08	1.502	0.04
490	1.000	0.00	1.000	0.00
510	0.838	0.03	0.878	0.01
555	0.652	0.05	0.713	0.03
620	1.110	0.06	0.930	0.06
670	1.611	0.11	1.204	0.11

The slope factors were derived from AC9 data that was measured during field campaigns in June 2001 and August 2002 (Kratzer & Tett, in press). The data set was divided up into I) outer fjord & open sea stations (B1–BY31 & H2), and II) inner fjord stations (H3–H4).

matter, TSM according to the terminology used in the MERIS protocols) and CDOM (yellow substance according to MERIS protocols). The latter has been chosen because initial tests showed that the IPF 4.10 does not produce good results in coastal waters. ESA has recently reprocessed the Reduced Resolution data with an improved version of the standard processor (MEGS 7.4), but for this study FR data were not available with that quality. The FUB Algorithm is a one step coupled atmospheric correction and water constituent retrieval method, implementing the inversion of a radiative transfer model by approximation with a neural network (Schroeder, 2005; Schroeder et al., 2002). Initial tests have shown that the results of the FUB algorithm in the coastal zone are more realistic than the IPF 4.10 level 2 data.

In order to compare the performance of the FUB Case-2 Plug-In to the new standard processor (MEGS 7.4), we

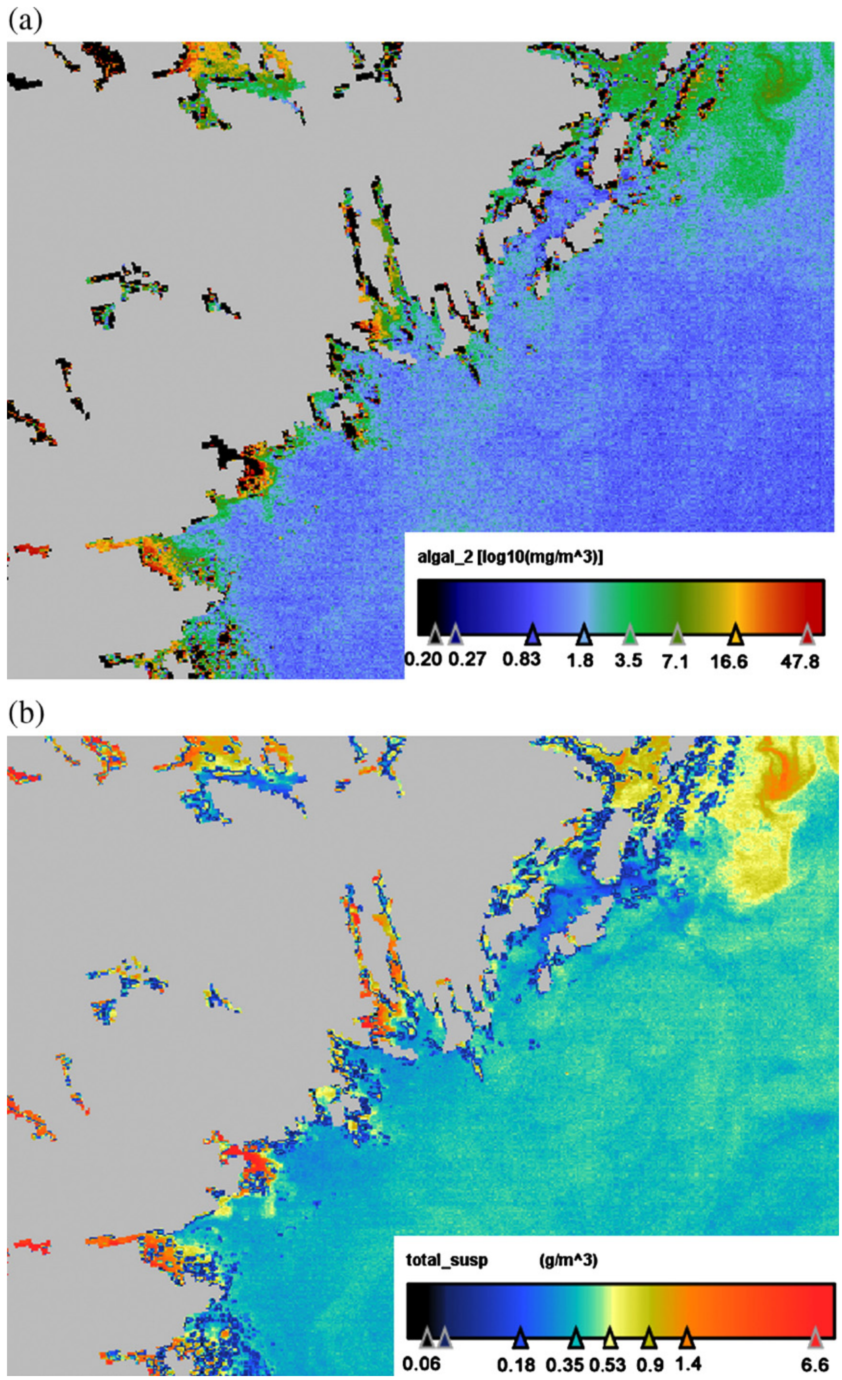

Fig. 4. (a) Chlorophyll concentration (algal-2 algorithm and (b) Suspended particulate matter (SPM, also termed total suspended matter, TSM) concentration derived from MERIS full resolution data from 19 August 2002. The level 1b processor was IPF 4.10, and for level 2 processing the FUB Case-2 Plug-In was used. The image shows that the sewage treatment plant does not act directly as a point source.

Please cite this article as: Kratzer, S., et al., Using MERIS full resolution data to monitor coastal waters — A case study from Himmerfjärden, a fjord-like bay in the northwestern Baltic Sea, *Remote Sensing of Environment* (2007), doi:10.1016/j.rse.2007.10.006

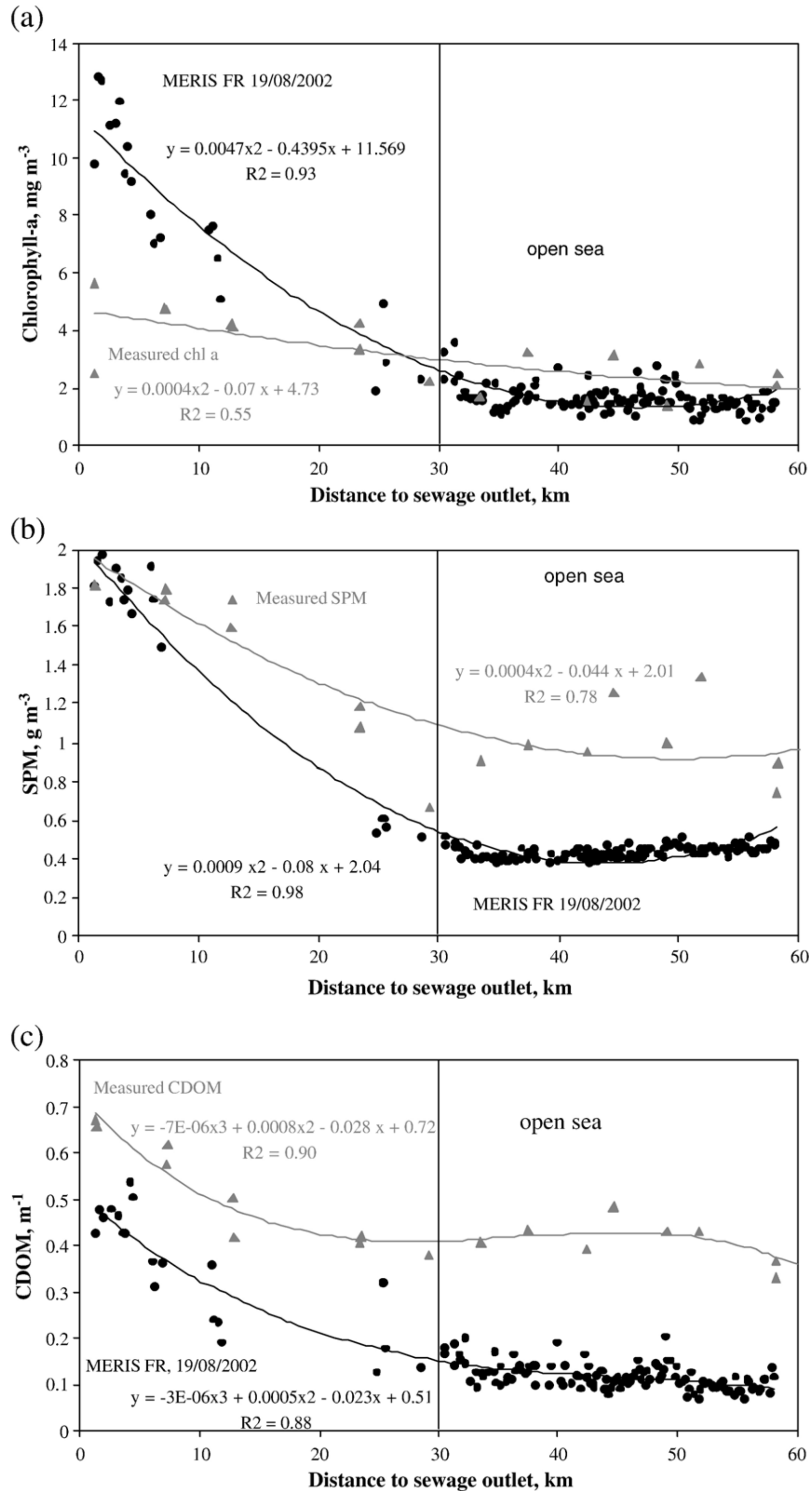

Fig. 5. (a) Chlorophyll *a*, (b) SPM (TSM) and (c) CDOM (yellow substance) transects derived from MERIS FR data from 19 August 2002 (FUB Case-2 Plug-In; level 1 processor: IPF 4.10) and plotted against distance to the outlet of the sewage treatment plant (satellite data: dark diamonds). In order to check the validity of this data, the sea-truthing data along the transect from August 2002 was plotted on the same diagram for each optical component (light grey triangles in Fig. 5 a–c). The distribution of chlorophyll and SPM was best described by a 2nd order polynomial, and the distribution of CDOM by a 3rd order polynomial, verifying the diffusional model described in Kratzer and Tett (in press). There is an off-set between satellite and sea-truthing trendline that can be approximated by deriving the off-set as the mean distance between the trendlines in the open Baltic Sea.

Please cite this article as: Kratzer, S., et al., Using MERIS full resolution data to monitor coastal waters — A case study from Himmerfjärden, a fjord-like bay in the northwestern Baltic Sea, *Remote Sensing of Environment* (2007), doi:10.1016/j.rse.2007.10.006

processed reduced resolution images from 16, 19, and 22 August 2002, both with the Case-2 Plug-In and with MEGS 7.4, and compared the results of both processors to sea-truthing data.

For the processing of MERIS data we used BEAM Version 3.6 — the Basic ENVISAT Toolbox for MERIS. BEAM includes VISAT, which is an open source desktop application for visualization, analyzing and processing of Envisat MERIS, AATSR, ASAR, ERS ATSR and also MODIS data. Both BEAM and the FUB Case-2 Plug-In can be downloaded freely from the BEAM Project home page: http://www.brockmann-consult.de/beam/.

A transect line was extracted from each of the level 2 products following the coordinates from the field campaign stations. For this the positions of the sea-truthing stations were used to mark the corresponding pixels in the image, which were then connected by straight lines in the image to define the transect. The pixel values for chlorophyll *a*, CDOM and SPM along this polyline were extracted, and the horizontal distance to the outlet of the sewage treatment plant was calculated for each pixel. Note: the outlet of the sewage treatment plant was used as a nominal starting point of the transect as elevated concentrations of bio-optical constituents may be expected there.

3. Results

The Baltic Sea belongs to those Case-2 waters that are highly dominated by CDOM. Only two measured SPM concentrations during the sea-truthing campaigns in 2001 and 2002 were below the threshold for Case-2 waters (0.5 g m^{-3}). However, the lowest CDOM concentrations measured were about ten times higher the threshold for Case-2!

As an example for the distribution of optical variables, Fig. 4 shows the distribution of (a) chlorophyll *a*, and (b) SPM derived from MERIS full resolution data using the FUB Case-2 Plug-In. Both images show that there is little fluvial input along this part of the Swedish coast, and that compared to the other coastal bays Himmerfjärden has no excessive output of SPM or chlorophyll to the open Baltic Sea. On contrary, there are some higher concentrations of both constituents shown further off-shore, which most likely are due to the occurrence of filamentous cyanobacteria, which were also observed at each station by pure eye both in the sea water as well as in the sampling bucket.

Despite the fact that we had especially planned these field campaigns for the sea-truthing of satellite data we only got a very limited number of real match-up data ($n=4$), and these were limited to inside Himmerfjärden. This is why, in the following, we use the trendlines of each optical component measured along the transects from August 2002 as sea-truthing reference for the satellite data.

The results of the transect analysis of the FR MERIS data are shown in Fig. 5 for (a) chlorophyll, (b) for SPM, and (c) for CDOM. In these plots, the sea-truthing data from the transects in August 2002 (grey triangles) are plotted against the distance to the sewage treatment outlet as a nominal reference point, whilst the satellite-derived data (from one individual overpass) are plotted on the same diagrams as black diamonds. The trend equations shown in each plot show the best polynomial fit for each component derived from the satellite data (black trend line), as well as the trendline of the sea-truthing data measured over August 2002 (grey line).

All constituents show a very clear polynomial trend, as predicted by the diffusion model described in Kratzer and Tett (in press). The distribution of chlorophyll and SPM was best described by a 2nd order polynomial (for chlorophyll there was no significant difference between a first order and a second order polynomial), and the distribution of CDOM by a 3rd order polynomial, which verifies the findings of the diffusional model.

This comparison between the MERIS FR and the sea-truthing data (Table 3) shows that total SPM was underestimated by about 50% in the open Baltic Sea and by about 16% in the coastal areas. CDOM was underestimated by about 74% in the open Baltic Sea, and about 37% in the coastal areas. Chlorophyll *a* was underestimated by about 35% in the open Baltic Sea, and overestimated by about 91% in the coastal areas when comparing to the trendline derived from all transect data measured during August 2002. For the open Baltic Sea data, the precision of the processor was relatively high (Standard deviation: 6–17%). However, we would like to point out that we measured maximum concentrations of all optical constituents during the satellite overpass on 19 August 2002 at station Hållvastö (northwest of Askö, about 15 km west of the transect) with a chlorophyll *a* concentration of 11.64 μg m^{-1}, SPM concentrations of 2.65 g m^{-3}, and CDOM attenuation of 0.77 m^{-1}. This may indicate that, the increased concentrations of optical constituents in the coastal regions, compared to the sea-truthing trendline may, indeed, have been caused by a sudden phytoplankton bloom event.

Fig. 6 shows the result of reduced resolution data from the open Baltic Sea processed with the standard processor (MEGS 7.4) and the FUB Case-2 Plug-In, respectively, in comparison to sea-truthing data. The trendline of the sea-truthing data (grey triangles) is shown in grey. The comparison of the RR data to the sea-truthing data show that, in the open Baltic Sea, the MERIS standard processor, on average, overestimated chlorophyll by about 59%, and SPM by about 28%, and underestimated yellow substance by about 81%, whereas the FUB

Table 3
MERIS FR transect: performance of FUB Case-2 processor in percent difference from sea-truthing data (deviation from polynomials plotted in Figs. 5a–c, 7 and 9; data set divided into coastal (0–30 km distance to STP), and open sea (30–60 km distance to STP)

	Distance	% Diff.	Chl *a* [a]	G_{440} [a]	SPM [a]	K_d (490) [b]	Inv. Secchi [b]
Coastal	0–30 km	Mean	91	−37	−16	0	0
		SD	67	17	23	11	6
Open sea	30–60 km	MEAN	−35	−74	−50	16	0
		SD	17	7	6	16	8

Note the K_d(490) and Secchi depth algorithms have been corrected for the off-set (sensitivity analysis).
[a] FUB product, not corrected for off-set.
[b] New algorithm, corrected for off-set.

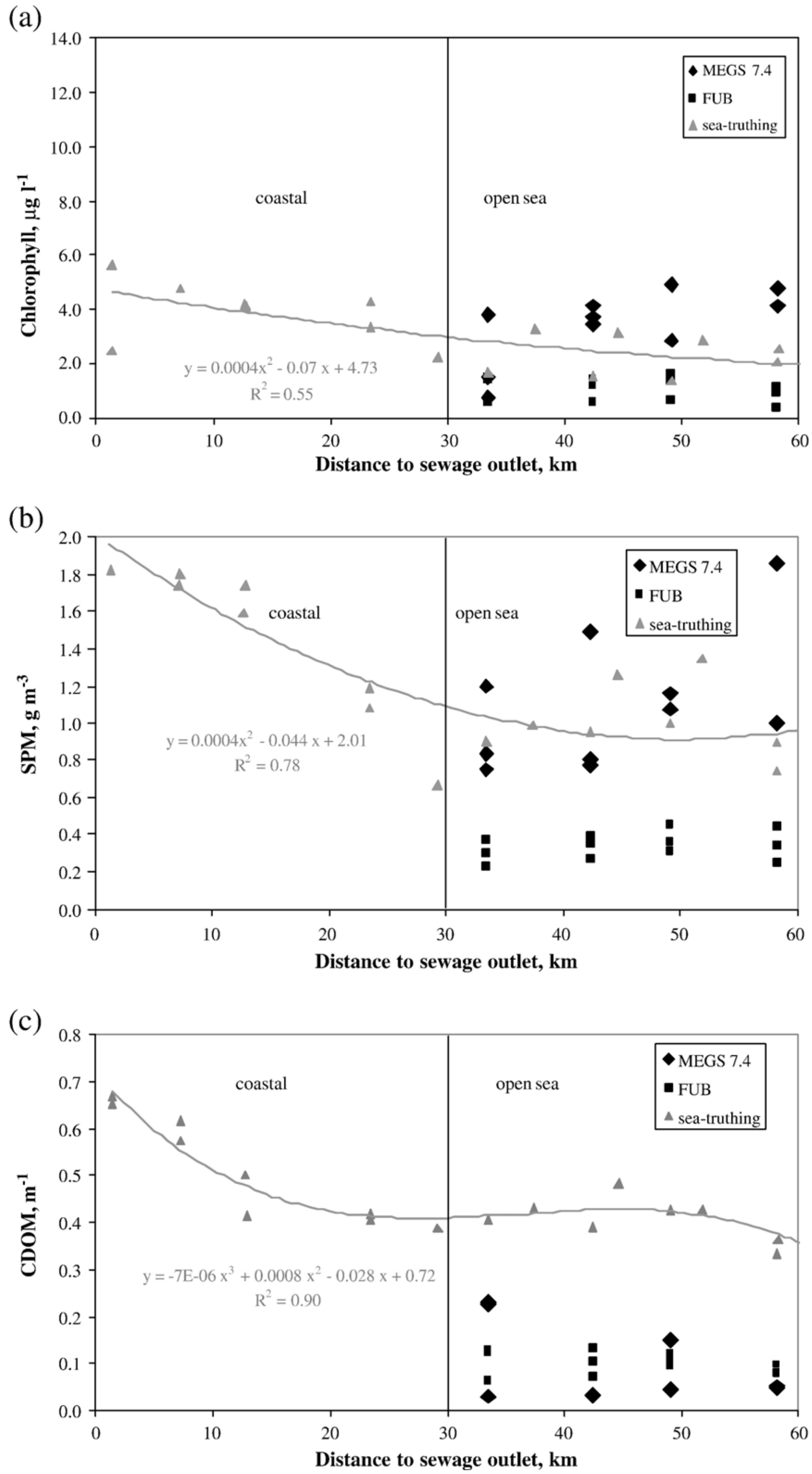

Fig. 6. (a) Chlorophyll *a*, (b) SPM (TSM) and (c) CDOM (yellow substance) data derived from MERIS RR data from 16, 19 and 22 August 2002 processed with the MEGS 7.4 (black diamonds) and the FUB Case-2 Plug-In (black squares) and plotted against distance to the outlet of the sewage treatment plant. In order to check the validity of this data, the sea-truthing data along the transect from August 2002 was plotted on the same diagram for each optical component (grey triangles and trendline). There is an off-set between satellite data and the sea-truthing trendline for each optical constituent that can be approximated by deriving the distance of the satellite trendline to the sea-truthing trendline.

processor underestimated SPM by about 60%, CDOM by about 78%, and chlorophyll *a* by about 56% (Table 4). The FUB processor showed a rather high precision for all optical components (6–18% standard deviation), whereas the precision for the MEGS 7.4 was rather low (43–73% standard deviation), except for CDOM (13% standard deviation).

Table 4
MERIS RR data: performance of standard processor (MEGS 7.4) and FUB Case-2 processor in percent difference from sea-truthing data (deviation from polynomials plotted in Fig. 5b)

Processor	RR data	Chl *a*	G_{440}	SPM
MEGS 7.4	Mean	59	−81	28
	SD	72	18	43
FUB	Mean	−56	−78	−60
	SD	18	6	10

3.1. Algorithm development

Initial tests showed that the best fit between the respective ln-transformed reflectance ratio and ln $[K_d(490)-K_dw]$ was obtained when using the reflectance ratios at 490 to 620 nm (corresponding to MERIS channel 3 and 6). The same was true when relating ln-transformed reflectance ratio to inverse and ln transformed Secchi depth data.

The $K_d(490)$ algorithm that yielded the best result for all data from 2002 (n=23) was:

$$\ln\,(K_d(490)-K_dw) \\ =-1.03{*}[\ln(\rho_{490}/\rho_{620})]-0.43;\quad r^2=0.84$$

If we use the data from cruises in 2000, 2001 and 2002 in the northwestern Baltic Sea (n=54), we get the following algorithm:

$$\ln\,(K_d(490)-K_dw) \\ =-1.17{*}[\ln(\rho_{490}/\rho_{620})]-0.51;\quad r^2=0.70$$

As a validity check, the satellite-derived $K_d(490)$ data for the MERIS FR scene from 19 August (using the algorithm for 2002) was compared to the $K_d(490)$ transect data measured over August 2002 (Table 1). Sensitivity analysis showed that there was a consistent off-set of about 0.25 m^{-1} between the satellite-derived and the measured $K_d(490)$ data, and the algorithm was therefore adjusted by adding 0.25 m^{-1}:

$$\ln\,(K_d(490)-K_dw)=-1.03{*}[\ln(\rho_{490}/\rho_{620})]-0.18$$

Fig. 7 shows the comparison between sea-truthing data (transects over the month of August) and the transect extracted from the MERIS scene from the 19 August 2002, using the adjusted $K_d(490)$ algorithm. Fig. 8 a shows a MERIS FR image from 22 August 2002 for which we used this algorithm on FUB-derived reflectances. The comparison between the satellite-derived and measured $K_d(490)$ data from the 22 August 2002 showed a strong correlation between predicted and measured data (r=0.94), as shown in Fig. 8 b; but the values tend below the 1:1 line.

The Secchi depth algorithm that yielded the best result for all Secchi data from 2002 (n=23) was:

$$\ln\,(\text{Secchi})=-1.32{*}\ln(\rho_{490}/\rho_{620})-1.27;\quad r^2=0.86,$$

and for the whole data set (2000–2002):

$$\ln\left(\text{Secchi}^{-1}\right)=-1.44*\ln(\rho_{490}/\rho_{620})-1.27;\quad r^2=0.79$$

4. Discussion

4.1. $K_d(490)$ algorithm

Mueller (2000) used the reflectance ratio 490:555 to derive $K_d(490)$ from SeaWiFS. MERIS does note have a channel at 555 nm, but at 560 nm instead. During the algorithm development we found that the 490:620 reflectance ratio scored almost the same coefficient of determination with an r^2 of 0.84 of $K_d(490)$ as the 490:560 ratio, which had an r^2 of 0.83 (n=23). However, when including data from cruises in 2000 and 2001 (n=58), the 490:620 reflectance ratio still scored an r^2 of 0.67, whereas the 490:560 ratio scored an r^2 of only 0.18

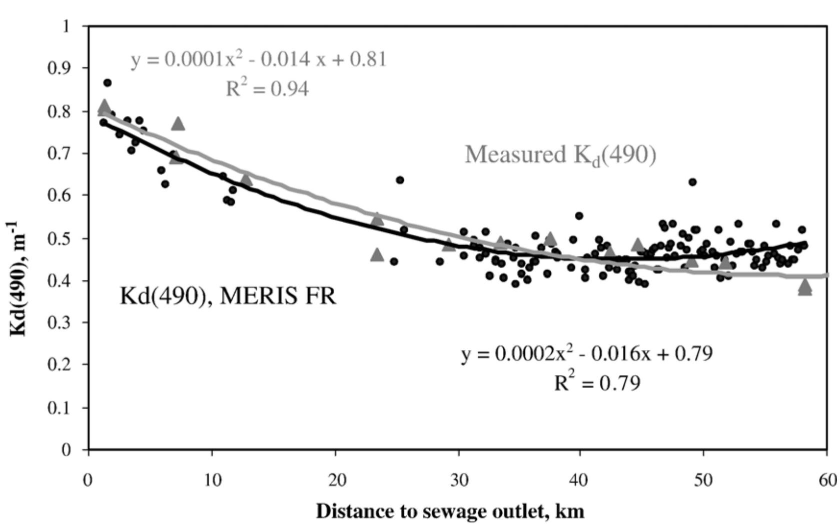

Fig. 7. A new K_d490 algorithm based on MERIS channel 3 (490 nm) and channel 6 (620 nm) was derived from radiometric sea-truthing data (TACCS, Satlantic) from 2002, and applied to the MERIS FR level 1b data (IPF 4.10 processor). The best algorithm used MERIS channel 3 (490 nm) and 6 (620 nm). The algorithm was then corrected for the off-set from the sea-truthing data by adding 0.25 m^{-1}. Black dots: $K_d(490)$ transect extracted from MERIS full resolution (FR) data (300 m resolution) registered on 19 August 2002. Grey triangles: measured K_d490 transect data over August 2002 (the measuring dates are given in Table 1). Note: both the satellite and sea-truthing trendline follow a polynomial decline from source to sink.

Please cite this article as: Kratzer, S., et al., Using MERIS full resolution data to monitor coastal waters — A case study from Himmerfjärden, a fjord-like bay in the northwestern Baltic Sea, *Remote Sensing of Environment* (2007), doi:10.1016/j.rse.2007.10.006

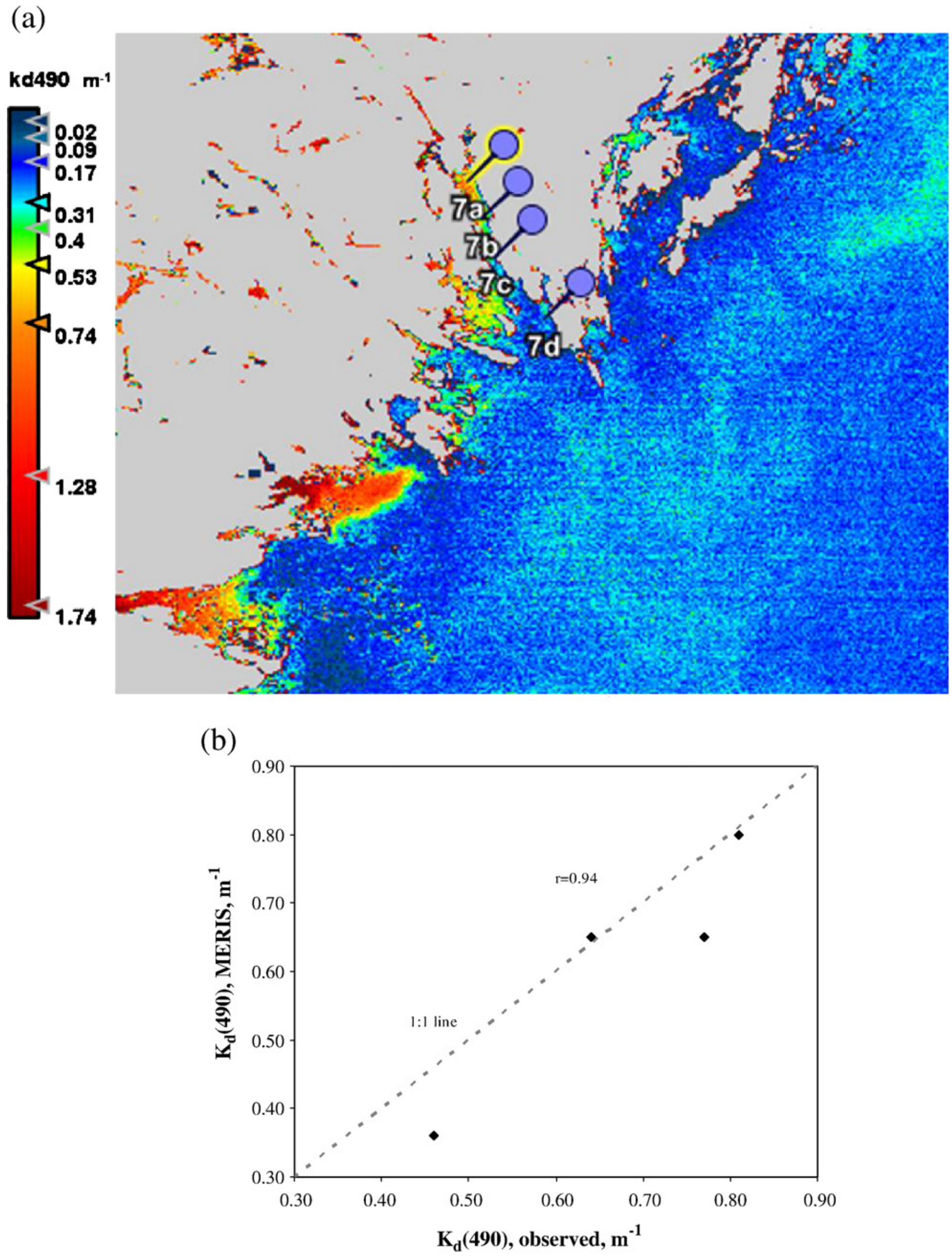

Fig. 8. (a) MERIS K_d(490) full resolution image (300 m resolution) from 22 August 2002 processed using BEAM and the K_d(490) algorithm derived using the sensitivity analysis. Stations (PINS) 7a–7b–7c–7d from head to mouth of Himmerfjärden which corresponds to the national monitoring stations H5-H4-H3-H2. (b) Comparison of the sea-truthing data from 22 August 2002 and satellite data extracted from the MERIS K_d(490) full resolution image in (a).

($n=58$). This may be due to variation in CDOM absorption that may still have a significant influence on the absorption spectrum at 555 nm (Kratzer, 2000). This means, that the algorithm using the reflectance ratio at 490:620 is more robust and should be valid for summer seasons in the northwestern Baltic Sea. Note that the algorithm is strictly only valid in the area of investigation, but it can be expected to work in the same salinity range as salinity is inversely correlated to CDOM which is the main optical component influencing the attenuation in the Baltic Sea (Kratzer & Tett, in press, Pierson et al., 2007).

The spectral diffuse attenuation coefficient, K_d(490) is important in itself as it can be used to determine the light conditions for phytoplankton or phytobenthic growth, and therefore can be used as input into productivity models. It has also been shown that K_d(490) can be estimated reliably from remote sensing observations in the Baltic Sea (Darecki & Stramski 2004; Kratzer et al., 2003). Our new K_d(490) algorithm confirms these findings, as it gives a good result when comparing to sea-truthing data (Fig. 8). The corrected K_d (490) algorithm that we derived via sensitivity analysis shows both a relatively good accuracy, and a relatively good precision (Table 3). Using K_d(490) we have a link between laborious measurements of in-water properties and a variable that can in principle be easily mapped over wide areas. In order to provide a level 2 product that can be used reliably by the user community, we therefore recommend that ESA should consider

Please cite this article as: Kratzer, S., et al., Using MERIS full resolution data to monitor coastal waters — A case study from Himmerfjärden, a fjord-like bay in the northwestern Baltic Sea, *Remote Sensing of Environment* (2007), doi:10.1016/j.rse.2007.10.006

including the spectral attenuation coefficient as a standard product of MERIS. However, as algorithms tend to be local, it is important to provide the used algorithm to the user community. In the framework of the GSE MarCoast project, for example, the diffuse attenuation coefficient is a parameter that is given to users, but the used algorithm is not published, which is a major drawback.

4.2. Secchi algorithm

The Secchi depth is inversely related to $K_d(490)$ (Kratzer et al., 2003) and therefore both the Secchi and the $K_d(490)$ algorithm with the best coefficient of determination were based on the same reflectance ratios, using the reflectances at 490 and 620 nm. Similar to the results for the $K_d(490)$ algorithm, the reflectance ratio at 490:560 also gave a good result for the data set from 2002 only (r^2 of 0.78), but not for the whole data set from 2000–2002; here the r^2 yielded only 0.23. This means that as for the $K_d(490)$, the reflectance ratio at 490:620 is more robust than the one at 490:560. Deriving a Secchi algorithm for satellite data is interesting from a historical perspective, as it provides a link between the relatively new satellite method, and one of the oldest measurements used in oceanography. There is also a large Secchi data set available in the Baltic Sea from standard monitoring stations, which can be used for verifying satellite data.

The comparison of MERIS-derived Secchi data (using the new algorithm derived from the TACCS measurements) to the sea-truthing data from 19 August 2002 showed that there was a rather consistent off-set in the open Baltic Sea. Sensitivity analysis showed that this off-set was about 0.11. If we correct for this off-set by adding 0.11 to the in-water algorithm, we can derive the following algorithm for MERIS:

$$\ln(\text{inverse Secchi}) = -1.32 * \ln(\rho_{490}/\rho_{620}) - 1.16$$

Fig. 9 shows the comparison between satellite-derived and measured Secchi depth using this algorithm (image from 19 August 2002). Table 3 shows that the MERIS-derived Secchi data using this algorithm compares very well with the sea-truthing data, both in coastal and open sea areas, and Fig. 10 shows a map of inverse Secchi depth derived for the 22 August 2002. The correlation coefficient for the four stations (7a–7d) was 0.75, also placed somewhat below the 1:1 line. More work has to be done to test this algorithm on an independent data set, including satellite scenes from other times of year.

4.3. Off-set between satellite and sea-truthing data

The initially observed off-set between the satellite-derived and the measured $K_d(490)$ and Secchi data may be due to problems with the atmospheric correction over coastal waters, and maybe to some extent due to environmental effects (adjacency effects) within the bay. Fig. 5c shows that there is a similar off-set between the satellite-derived and measured CDOM attenuation. As most of the attenuation in Baltic Sea water is caused by CDOM (Kratzer & Tett, in press), a similar off-set may also be expected for the diffuse attenuation coefficient. The off-set in all water products is most likely related to inaccuracies in the atmospheric model (personal communication with Jürgen Fischer, June 2007). Fig. 11 shows the comparison between the MERIS-derived reflectances (FUB processor) and the reflectances derived from the TACCS transect data from 22 August 2002 (station H5–H2). The MERIS reflectances are too high across the whole spectrum. Furthermore, the spectral shape is wrong in the blue and the reflectances in the blue are too high in relation to the other bands, which is a sign of an over-correction of atmospheric effects. The FUB Case-2 Plug-In for BEAM solves an atmospheric model and an in-water model simultaneously (Schroeder, 2005; Schroeder et al., 2002), which means that an inaccuracy in one part of the model will lead to an inaccuracy in the other part of the model. This is probably the explanation as to why the water products were all underestimated in the open Baltic Sea. (Fig. 5).

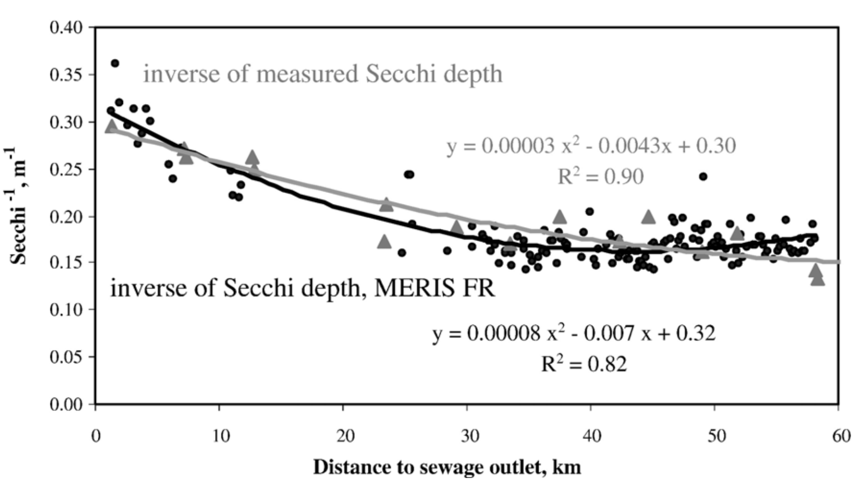

Fig. 9. Inverse Secchi depth derived from MERIS data from 19 August 2002 using the new algorithm. In order to derive the algorithm, the natural logarithm the inverse Secchi depth was plotted against the natural logarithm of various combinations of reflectance ratios (n=23). The reflectance ratio that yielded the highest coefficient of determination (r^2) in this test was then chosen as the best algorithm. Similar to the results for the $K_d(490)$ algorithm the best algorithm was derived when using MERIS channel 3 (490 nm) and 6 (620 nm). The algorithm was corrected for the off-set from the sea-truthing data by adding 0.11.

Please cite this article as: Kratzer, S., et al., Using MERIS full resolution data to monitor coastal waters — A case study from Himmerfjärden, a fjord-like bay in the northwestern Baltic Sea, *Remote Sensing of Environment* (2007), doi:10.1016/j.rse.2007.10.006

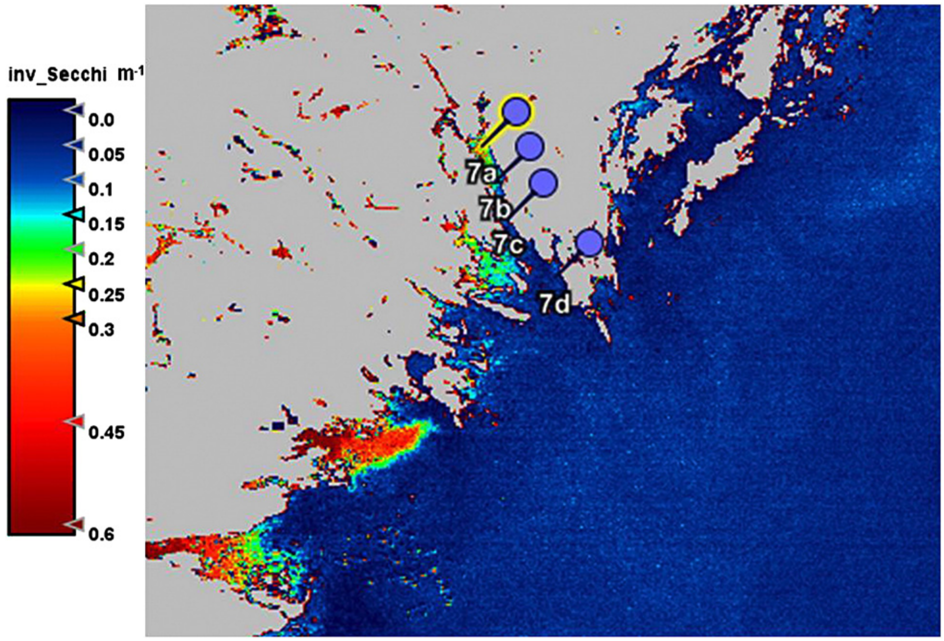

Fig. 10. Inverse Secchi depth (m^{-1}) map as derived from the MERIS scene from 22 August 2002, using the adjusted Secchi depth algorithm derived from the whole data set from 2002.

The NASA Aeronet project has a world-wide network of Cimel sun photometers, which measure the spectral signature of aerosols, from which one can derive e.g. aerosol optical thickness and the Ångström coefficient. In collaboration with Stockholm University, the Swedish Meteorological and Hydrological Institute (SMHI) has been maintaining an Aeronet station in Sweden since 2000 (Carlund et al., 2005). The mean of the Ångström coefficient, α (440–870), derived from the SMHI Aeronet data over August 2002 was 1.53 ± 0.31, whereas the mean Ångström coefficient derived from the MERIS FR level 2 data (using the FUB Plug-In) was only 0.52 ± 0.07, and was therefore underestimated by about 66%. This supports our hypothesis that the observed off-set for $K_d(490)$ and the other level 2 products was caused by errors in the atmospheric correction. However, it should be noted as well that the FUB algorithm does not seem to be able to distinguish between chlorophyll and CDOM: the FUB level 2 product for yellow substance showed the same distribution as the chlorophyll map (algal_2 product) with the typical patterns of a predominant cyanobacteria community (see Fig. 4a). There was a strong correlation between log (chlorophyll) and log (CDOM) for the FUB product, which was not shown in the result of the standard product. The standard product showed increasing CDOM towards the land but showed also contrails (which is an indication of a failing atmospheric correction), and the image looked rather noisy.

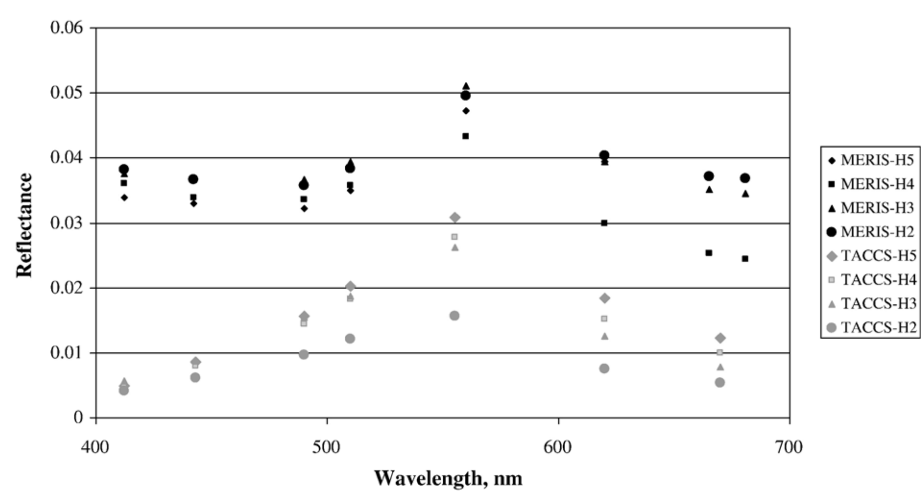

Fig. 11. Comparison of reflectances derived form TACCS (sea-truthing data) to reflectances derived from MERIS (FUB processor) across the Himmerfjärden transect from 22 August 2002 (satellite data extracted from MERIS full resolution image). The MERIS reflectances are too high across the whole visible spectrum. The shape of the MERIS reflectances is wrong in the blue which indicates a flaw in the atmospheric correction. Note that the sea-truthing reflectances are consistent with higher reflectances towards the head of the fjord, which can be explained with an increase in inorganic suspended particulate matter.

Please cite this article as: Kratzer, S., et al., Using MERIS full resolution data to monitor coastal waters — A case study from Himmerfjärden, a fjord-like bay in the northwestern Baltic Sea, *Remote Sensing of Environment* (2007), doi:10.1016/j.rse.2007.10.006

4.4. Relating optical properties spatially

Because of the frequent cloud cover over the Baltic Sea it is very difficult to get a temporal match between the satellite overpass and the sea-truthing data. Even though this study was especially aimed at validating satellite data, we only got a very limited number of real match-ups ($n=4$). The use of optical transects along optical gradients proved here to be very useful for the sea-truthing of FR MERIS data (Figs. 5 and 6). By relating the sea-truthing and the satellite data to distance to the shore one has an additional reference-value for the measured satellite data as the concentrations do not only differ over time, but also over space (Kratzer & Tett, in press). The comparison of the satellite-derived $K_d(490)$ measurements to the transects measured over August 2002 strengthens this argument. There is a remarkable fit between the two data sets, even though the measured data represents the mean over the month August, and the satellite data was registered over seconds. In order to evaluate if the satellite data are in the right range of values, one may therefore not need exact match-ups, but data from the same season that is related to the distance to the shore. In this way one may overcome some of the practical problems related to the frequent cloud cover over the Baltic Sea area.

The results in Figs. 4a–b, 8a and 10 show that the spatial resolution of MERIS FR data is sufficient to monitor changes of water quality in coastal areas. The distribution of chlorophyll and SPM was best described by a 2nd order polynomial, and the distribution of CDOM by a 3rd order polynomial, which verifies the findings of the diffusional model described in Kratzer and Tett (in press) (Fig. 5 a–c). This clearly adds additional confidence to the results of the satellite data.

Branco and Kremer (2005) emphasized the role of CDOM to the prediction of the diffuse attenuation coefficient, and therefore to the productivity of small estuaries. Because CDOM absorbs mostly in the blue light of the spectrum it preferentially removes light that is critical for photosynthesis, and therefore may limit the productivity. Branco and Kremer (2005) suggest that the next step towards quantitative assessment is to move from measuring CDOM to an ability to predict its distribution. We have done this here on a local scale both by relating our sea-truthing CDOM data to distance from the shore as well using MERIS full resolution imagery.

The validation of the satellite-derived CDOM showed that CDOM has a rather high precision for both processors, both in the open sea and the coastal areas. It should be possible to use both the standard processor (MEGS 7.4) and the FUB algorithm to derive CDOM, if the off-set is corrected for with measured data (Tables 3 and 4, and Figs. 5c and 6c).

5. Conclusions

In summary, one may state that the precision of the satellite data improves by applying the FUB Case-2 processor and that the accuracy improves with better spatial resolution. The FUB processor can be used off-the-shelf for open Baltic Sea monitoring of all level 2 products, provided one corrects for the respective off-set from the measured sea-truthing data that is most likely caused by an inaccuracy in the atmospheric correction. Additionally, the FUB processor appears to be able to derive CDOM, $K_d(490)$ and Secchi depth in Himmerfjärden (also provided one corrects for the respective off-set). The results of the new $K_d(490)$ algorithm look very promising. However, we will need to perform more comparisons between sea-truthing and MERIS FR data before the new $K_d(490)$ and Secchi algorithms can be made operational, including also scenes from other times of year. In order to provide a level 2 product that can be used reliably by the user community in the Baltic Sea, we recommend that ESA should consider including the spectral attenuation coefficient as a standard product of MERIS. The new *MERIS Case-2 Regional Processor* developed by Doerffer et al. (2006) provides such a product, and we are planning to compare the performance of this product to the results of our own $K_d(490)$ algorithm. ESA is currently working on a better instrument calibration and on an improvement of the MERIS atmospheric correction and it will be interesting to see if this will also improve the accuracy of the standard water products. The new version of the standard processor is planned to be released in 2008.

Acknowledgements

This work was funded by the Swedish National Space Board, by ESA under the ENVISAT programme, and by the EU FP6 Integrated Project SPICOSA (Science and Policy Integration for Coastal System Assessment). Thanks to NASA for providing us with SeaWiFS quick-looks during field campaigns.

The authors thank Stefanie Hirch, Roberta Mistretta, Antonia Sandman and Charlotte Sahlin for their assistance in the field and in the laboratory. Thanks to Henrik Lindh (SMHI) and the staff from Askö Laboratory for the invaluable support during fieldwork. We are grateful to the reviewers for their helpful comments on the manuscript.

References

Antoine, D., & Morel, A. (2000). Atmospheric correction over the ocean (Case 1 waters). ESA Document ATBD 2.7, Doc. No.: PO-TN-MEL-GS-0005, Laboratoire de Physique et Chimie Marines.

Bowers, D. G., Harker, G. E. L., Smith, P. S. D., & Tett, P. (2000). Optical properties of a region of freshwater influence (The Clyde Sea). *Estuarine, Coastal and Shelf Science*, *50*, 717−726.

Branco, A. B., & Kremer, J. N. (2005). The Relative Importance of Chlorophyll and Colored Dissolved Organic Matter (CDOM) to the prediction of the diffuse attenuation coefficient in Shallow Estuaries. *Estuaries*, *28*(5), 643−652.

Carlund, T., Hakansson, B., & Land, P. (2005, Jan 20). Aerosol optical depth over the Baltic Sea derived from AERONET and SeaWiFS measurements. *International Journal of Remote Sensing*, *26*(2), 233−245.

Darecki, M., & Stramski, D. (2004). An evaluation of MODIS and SeaWiFS bio-optical algorithms in the Baltic Sea. *Remote Sensing Environment*, *89*, 326−350.

Doerffer, R. (2002). Protocols for the validation of MERIS water products. European Space Agency Doc. No. PO-TN-MEL-GS-0043.

Doerffer, R., & Schiller, H. (2006). The MERIS Neural Network Algorithm. Chapter 6. In: Remote sensing of inherent optical properties: fundamentals, tests of algorithms, and applications. In Z. -P. Lee (Ed.), Reports of the International Ocean-Colour Coordinating Group, No. 5, IOCCG, Dartmouth, Canada.

Doerffer, R., Sorensen, K., & Aiken, J. (1999). MERIS potential for coastal zone application. *International Journal of Remote Sensing*, *20*(9), 1809−1818.

Doerffer, R., Schiller, H., & Peters, M. (2006). The Meris Case-2 Regional processor, version 1.1, published 8 November 2006 on http://www.brockmann-consult.de/beam/plugins.html.

Engqvist, A. (1996). Long-term nutrient balances in eutrophication of the Himmerfjärden estuary. *Estuarine, Coastal and Shelf Science*, *42*, 483−507.

Gordon, H. R. (1973). Simple calculation of the diffuse reflectance of the ocean. *Applied Optics*, *12*, 2803−2804.

Gordon, H. R., & Morel, A. Y. (1983). Remote assessment of ocean colour for interpretation of satellite visible imagery: A review. New York: Springer Verlag.

Gordon, H. R., & Wang, M. (1994). Retrieval of water-leaving radiance and aerosol optical thickness over the oceans with SeaWiFS: A preliminary algorithm. *Applied Optics*, *33*, 443−452.

Højerslev, N. K., Holt, N., & Aarup, T. (1996). Optical measurements in the North Sea–Baltic Sea transition zone. I. On the origin of deep water in the Kattegat. *Continental Shelf Research*, *16*(10).

Jeffrey, S. W., & Humphrey, G. F. (1975). New spectrophotometric equation for determining chlorophyll a, b, c1 and c2. Biochemie und Physiologie der Pflanzen, *167*, 194−204.

Jeffrey, S. W., Matoura, R. F. C., & Wright, S. W. (1997). *Phytoplankton pigments in oceanography.* UNESCO Publishing.

Jerlov, N. G. (1951). Optical studies of ocean water. Reports of the Swedish Deep-Sea Expedition, *3*, 1−59.

Jerlov, N. G. (1976). Marine optics.Amsterdam: Elsevier 231 pp.

Kirk, J. T. O. (1994). *Light and photosynthesis in aquatic ecosystems*, 2nd Edition UK: Cambridge University Press 509 pp.

Kratzer, S. (2000). *Bio-optical studies of coastal waters.* PhD thesis, monograph, School of Ocean Sciences.Bangor, UK: University of Wales 190 pp.

Kratzer, S., & Tett, P., (in press). Using bio-optics to investigate the extent of coastal waters — A Swedish case study. Hydrobiologia.

Kratzer, S., Bowers, D. G., & Tett, P. (2000). Seasonal changes in colour ratios and optically active constituents in the optical Case-2 waters of the Menai Strait, North Wales. *International Journal of Remote Sensing*, *21*(11), 2225−2246.

Kratzer, S., Håkansson, B., & Sahlin, C. (2003). Assessing Secchi and photic zone depth in the Baltic Sea from satellite data. *Ambio*, *32*, 577−585.

Kratzer, S., Moore, G.F., & Martinez Vicente, V., Bio-optical relationships in the Baltic Sea and other European coastal waters, in preparation for Limnology & Oceanography.

Lavender, S. J., Pinkerton, M. H., Moore, G. F., Aiken, J., & Blondeau-Patissier, D. (2005). Modification to the atmospheric correction of SeaWiFS ocean colour images over turbid waters. *Continental Shelf Research*, *25*(4), 539−555.

Moore, G. F., & Aiken, J. (2000). Case 2 (s) bright pixel atmospheric correction. Algorithm Theoretical Basis Document, ATBD 2.6. MERIS ESL Doc. No: PO-TN-MEL-GS-0005: http://envisat.esa.int/instruments/meris/pdf/atbd_2_06.pdf

Moore, G. F., Aiken, J., & Lavender, S. J. (1999). The atmospheric correction of water colour and the quantitative retrieval of suspended particulate matter in Case II waters: Application to MERIS. *International Journal of Remote Sensing*, *20*, 1713−1733.

Morel, A., & Gentili, B. (1991). Diffuse reflectance of oceanic waters: its dependence on Sun angle as influenced by the molecular scattering contribution. *Applied Optics*, *30*, 4427−4438.

Morel, A., & Gentili, B. (1993). Diffuse reflectance of oceanic waters. II. Bi-directional aspects. *Applied Optics*, *32*, 6864−6879.

Morel, A., & Gentili, B. (1996). Diffuse reflectance of oceanic waters. III. Implication of bidirectionality for the remote-sensing problem. *Applied Optics*, *35*(24), 4850−4862.

Morel, A., & Prieur, L. (1977). Analysis of variations in ocean colour. *Limnology and Oceanography*, *22*, 709−722.

Mueller, L. J. (2000). SeaWiFS Algorithm for the diffuse attenuation coefficient, *K* (490), using water-leaving radiances at 490 and 555 nm. In S. B. Hooker, & E. R. Firestone (Eds.), SeaWiFS Postlaunch Calibration and Validation Analyses, Part 3, *11*. (pp. 24−27) Greenbelt, Maryland: NASA GSFC.

Mueller, J. L., & Austin, R. W. (1995). Ocean optics protocols for SeaWiFS validation, revision 1. In S. B. Hooker, E. R. Firestone, & J. G. Acker (Eds.), NASA Tech. Memo. 104566, *Vol. 25*. Greenbelt, Maryland: NASA Goddard Space Flight Center 66 pp.

Parsons, T. R., Maita, Y., & Lalli, C. M. (1984). *A manual of chemical and biological methods for seawater analysis.* Pergamon Press.

Pierson, D. C., Kratzer, S., Strömbeck, N., & Håkansson, B. (2007). Relationship between the attenuation of downwelling irradiance at 490 nm with the attenuation of PAR (400 nm–700 nm) in the Baltic Sea. *Remote Sensing of Environment*, doi:10.1016/j.rse.2007.06.009.

Preisendorfer, R. W. (1961). Application of radiative transfer theory to light measurements in the sea. *IUGG Monographs*, *10*, 11−30.

Sathyendranath, S., & Platt, T. (1997). Analytic model of ocean color. *Applied Optics*, *36*, 2620−2629.

Schroeder, T., (2005). Fernerkundung von Wasserinhaltsstoffen in Küstengewässern mit MERIS unter Anwendung expliziter und impliziter Atmosphärenkorrekturverfahren. Ph.D. Dissertation, Freie Universität Berlin, Berlin (Germany), 2005, http://www.diss.fu-berlin.de/2005/78

Schroeder, T., & Schaale, M. (2005). *MERIS* Case-2 Water Properties Processor, Version 1.0.1. Institute for Space Sciences, Freie Universität Berlin (FUB), http://www.brockmann-consult.de/beam/software/plugins/FUB-WeW-Water-1.0.1.zip

Schroeder, T., Fischer, J., Schaale, M., & Fell, F. (2002). Artificial neural network based atmospheric correction algorithm: Application to MERIS data. Proceedings of the International Society for Optical Engineering (SPIE), *Vol. 4892*. Hangzhou, China.

Siddorn, J. R., Bowers, D. G., & Hoguane, A. M. (2001). Detecting the Zambezi River plume using observed optical properties. Marine Pollution Bulletin, *42*, 942−950.

Smith, R. C., & Baker, K. S. (1981). Optical properties of the clearest natural waters (200–800 nm). *Applied Optics*, *20*, 177−184.

Stamnes, K., Li, W., Yan, B., Eide, H., Barnard, A., Pegau, W. S., et al. (2003). Accurate and self-consistent ocean color algorithm: Simultaneous retrieval of aerosol optical properties and chlorophyll concentrations. *Applied Optics*, *42*(6), 939−951.

Strickland, J. H. D., & Parsons, T. R. (1972). A practical handbook of sea-water analysis. *Bulletin Journal of the Fisheries Research Board of Canada*, *167*, 185−203.

Voipio, A. (1981). *The Baltic Sea.* New York: Elsevier Science Publishers.

WetLabs (2007, March). ac-meter Protocol Revision L, 13. http://www.wetlabs.com/products/pub/ac9/acprotl.pdf